

## Effect of Thermo-Diffusion and Chemical Reaction on Mixed Convective Heat And Mass Transfer Through A Porous Medium In Cylindrical Annulus With Heat Source.

Dr.K.Gnaneswar

Principal,S.KP.Government Degree College, Guntakal, Anantapuramu-(Dist), Andhra Pradesh-India

### Abstract:

A finite element study of combined heat and mass transfer flow through a porous medium in a circular cylindrical annulus with Soret and Dufour effects in the presence of heat sources has been analyzed. The coupled velocity, energy, and diffusion equations are solved numerically by using Galerkin- finite element technique. Shear stress, Nusslet number and Sherwood number are evaluated numerically for different values of the governing parameters under consideration and are shown in tabular form.

**Keywords:** Heat and mass transfer, Soret effect, Dufour effect, Constant heat source, and Chemical reaction.

### I. Introduction

Transport phenomena involving the combined influence of thermal and concentration buoyancy are often encountered in many engineering systems and natural environments. There are many applications of such transport processes in the industry, notably in chemical distilleries, heat exchangers, solar energy collectors and thermal protection systems. In all such classes of flows, the driving force is provided by a combination of thermal and chemical diffusion effects. In atmosphere flows, thermal convection of the earth by sunlight is affected by differences in water vapor concentration. This buoyancy driven convection due to coupled heat and mass transfer in porous media has also many important applications in energy related engineering. These include moisture migration, fibrous insulation, spreading of chemical pollution in saturated soils, extraction of geothermal energy and underground disposal of natural waste.

The increasing cost of energy has led technologists to examine measures which could considerably reduce the usage of the natural source energy. Thermal insulations will continue to find increased use as engineers seek to reduce cost. Heat transfer in porous thermal insulation with in vertical cylindrical annuli provides us insight into the mechanism of energy transport and enables engineers to use insulation more efficiently. In particular, design engineers require relationships between heat transfer, geometry and boundary conditions which can be utilized in cost-benefit analysis to determine the amount of insulation that will yield the maximum investment. Apart from this, the study of flow and heat transfer in the annular region between the concentric cylinders has applications in nuclear waste disposal research. It is known that canisters filled

with radioactive rays be buried in earth so as to isolate them from human population and is of interest to determine the surface temperature of these canisters. This surface temperature strongly depends on the buoyancy driven flows sustained by the heated surface and the possible moment of groundwater past it. This phenomenon is ideal to the study of convection flow in a porous medium contained in a cylindrical annulus.

Free convection in a vertical porous annulus has been extensively studied by Prasad [22], Prasad and Kulacki [23] and Prasad et al [24] both theoretically and experimentally. Caltagirone [5] has published a detailed theoretical study of free convection in a horizontal porous annulus including possible three dimensional and transient effects. Convection through annulus region under steady state conditions has also been discussed with two cylindrical surface kept at different temperatures [14]. This work has been extended in temperature dependent convection flow [8,9,14] as well as convection flows through horizontal porous channel whose inner surface in maintained at constant temperature while the other surface is maintained at circumferentially varying sinusoidal temperature [17,27,35].

Free convection flow and heat transfer in hydro magnetic case is important in nuclear and space technology [14, 20, 22, 30, 36, 37]. In particular, such convection flow in a vertical annulus region in the presence of radial magnetic field has been studied by Sastry and Bhadram [28]. Nanda and Purushotham [14] have analyzed the free convection of a thermal conducting viscous incompressible fluid induced by traveling thermal waves on the circumference of a long vertical circular cylindrical pipe. Whitehead

[35], Neeraja [15] has made a study of the fluid flow and heat transfer in a viscous incompressible fluid confined in an annulus bounded by two rigid cylinders. The flow is generated by periodical traveling waves imposed on the outer cylinder and the inner cylinder is maintained at constant temperature.

Chen and Yih [6] have investigated the heat and mass transfer characteristics of natural convection flow along a vertical cylinder under the combined buoyancy effects of thermal and species diffusion. Sivanjaneya Prasad [31] has investigated the free convection flow of an incompressible, viscous fluid through a porous medium in the annulus between the porous concentric cylinders under the influence of a radial magnetic field. Antonio [3] has investigated the laminar flow, heat transfer in a vertical cylindrical duct by taking into account both viscous dissipation and the effect of buoyancy, the limiting case of fully developed natural convection in porous annuli is solved analytically for steady and transient cases by E. Sharawi and Al-Nimir [29]. Philip [20] has obtained solutions for the annular porous media valid for low modified Reynolds number. Rani [25] has analyzed the unsteady convective heat and mass transfer through a cylindrical annulus with constant heat sources. Sreevani [33] has studied the convective heat and mass transfer through a porous medium in a cylindrical annulus under radial magnetic field with Soret effect. Prasad [22] has analyzed the convective heat and mass transfer in an annulus in the presence of heat generating source under radial magnetic field. Reddy [32] has discussed the Soret effect on mixed convective heat and mass transfer through a porous cylindrical annulus. For natural convection, the existence of large temperature differences between the surfaces is important. Keeping the applications in view, Sudheer Kumar et al [34] have studied the effect of radiation on natural convection over a vertical cylinder in a porous media.

In many industrial applications of transient free convection flow problems, there occurs a heat source or a sink which is either a constant or temperature gradient or temperature dependent heat source. This heat source occurs in the form of a coil or a battery. Gokhale and Behnaz-Farman analyzed Transient free convection flow of an incompressible fluid past an isothermal plate with temperature gradient dependent heat sources. Implicit finite difference scheme which is unconditionally stable has been used to solve the governing partial differential equations of the flow. Transient temperature and velocity profiles are plotted to show the effect of heat source. Sreevani [33] has analyzed the Soret effect on convective heat and mass transfer flow of a viscous fluid in a cylindrical annulus with heat generating sources.

There are few studies about the Soret and Dufour effects in a Darcy or non-Darcy porous medium. Angel et al [2] has examined the composite Soret and Dufour effects on free convective heat and mass transfer in a Darcian porous medium with Soret and Dufour effects. Postelnicu [19] has studied the heat and mass transfer characteristics of natural convection about vertical surface embedded in a saturated porous medium subjected to magnetic field by considering the Soret and Dufour effects. Partha et al. [18] have examined the Soret and Dufour effects in a non-Darcy porous medium. Mansour et al. [12] have studied the multiplicity of solutions induced by thermosolutal convection in a square porous cavity heated from below and submitted to horizontal concentration gradient in the presence of Soret effect. Lakshmi Narayana et al [10] have studied the Soret and Dufour effects in a doubly stratified Darcy porous medium. Lakshmi Narayana and Murthy [11] have examined the Soret and Dufour effects on free convective heat and mass transfer from a horizontal flat plate in a Darcy porous medium. Very recently Barletta, A, Lazzari, S and others [4] have studied on mixed convection with heating effects in a vertical porous annulus with a radially varying magnetic field. Emmunuel Osalusi, Jonathan Side, Robert Harris [7] have discussed Thermal-diffusion and diffusion thermo effects on combined heat and mass transfer of a steady MHD convective and slip flow due to a rotating disk with viscous dissipation and ohmic heating.

In this paper we discuss the free and forced convective heat and mass transfer of a viscous fluid flow through a porous medium in a circular cylindrical annulus with Thermal-Diffusion and Diffusion-Thermo effects in the presence of constant heat source, where the inner wall is maintained constant temperature while the outer wall is constant heat flux and the concentration is constant on the both walls. The Brinkman-Forchhimer extended Darcy equations which take into account the boundary and inertia effects are used in the governing linear momentum equations. The effect of density variation is confined to the buoyancy term under Boussinesque - approximation. The momentum, energy and diffusion equations are coupled equations. In order to obtain a better insight into this complex problem, we make use of Galerkin finite element analysis with quadratic polynomial approximations. The Galerkin finite element analysis has two important features. The first is that the approximation solution is written directly as a linear combination of approximation functions with unknown nodal values as coefficients. Secondly, the approximation polynomials are chosen exclusively from the lower order piecewise polynomials restricted to contiguous elements. The behavior of velocity, temperature and

concentration are analyzed for different parameters. The shear stress and the rate of heat and mass transfer have also obtained for variations in the governing parameters.

## II. Formulation of the problem:

We consider free and force convection flow through a porous medium in a circular cylindrical annulus with Thermal-Diffusion and Diffusion-Thermo effects in the presence of constant heat source, whose inner wall is maintained at a constant temperature and the outer wall is maintained constant heat flux also the concentration is constant on the both walls. The flow velocity, temperature and concentration in the fluid to be fully developed. Both the fluid and porous region have constant physical properties and the flow is a mixed convection flow taking place under thermal and molecular buoyancies and uniform axial pressure gradient. The bousseinessque approximation is invoked so that the density variation is confined to the thermal and molecular buoyancy forces. The Brinkman-Forchhiner-Extended Darcy model which accounts for the inertia and boundary effects has been used for the momentum equation in the porous region. In the momentum, energy and diffusion are coupled and non-linear. Also the flow in is unidirectional along the axial cylindrical annulus. Making use of the above assumptions the governing equations are

$$-\frac{\partial p}{\partial z} + \frac{\mu}{\delta} \left( \frac{\partial^2 u}{\partial r^2} + \frac{1}{r} \frac{\partial u}{\partial r} \right) - \frac{\mu}{k} u - \frac{\rho \delta F}{\sqrt{k}} u^2 + \rho g \beta (T - T_0) + \rho g \beta^* (C - C_0) = 0 \quad (2.1)$$

$$\rho c_p u \frac{\partial T}{\partial z} = \lambda \left( \frac{\partial^2 T}{\partial r^2} + \frac{1}{r} \frac{\partial T}{\partial r} \right) + Q + \frac{D_m K_t}{c_s c_p} \left( \frac{\partial^2 C}{\partial r^2} + \frac{1}{r} \frac{\partial C}{\partial r} \right) \quad (2.2)$$

$$u \frac{\partial C}{\partial z} = D_1 \left( \frac{\partial^2 C}{\partial r^2} + \frac{1}{r} \frac{\partial C}{\partial r} \right) + \frac{D_m K_t}{T_m} \left( \frac{\partial^2 T}{\partial r^2} + \frac{1}{r} \frac{\partial T}{\partial r} \right) - K_1 C \quad (2.3)$$

Where  $u$  is the axial velocity in the porous region,  $T$  &  $C$  are the temperature and concentrations of the fluid,  $k$  is the permeability of porous medium,  $F$  is a function that depends on Reynolds number and the microstructure of the porous medium and  $D_1$  is the Molecular diffusivity,  $D_m$  is the coefficient of mass diffusivity,  $T_m$  is the mean fluid temperature,  $K_t$  is the thermal diffusion,  $C_s$  is the concentration susceptibility,  $C_p$  is the specific heat,  $\rho$  is density,  $g$  is gravity,  $\beta$  is the coefficient of thermal expansion,  $\beta^*$  is the coefficient of volume expansion .

The boundary conditions relevant to

$$u = 0 \quad \& \quad T = T_i, \quad C = C_i \quad \text{at} \quad r = a \quad (2.4)$$

$$u = 0 \quad \& \quad \frac{\partial T}{\partial r} = Q_1, \quad C = C_0 \quad \text{at} \quad r = a + s \quad (2.5)$$

The axial temperature gradient  $\frac{\partial T}{\partial z}$  and concentration gradient  $\frac{\partial C}{\partial z}$  are assumed to be constant say A and B respectively.

we now define the following non-dimensional variables

$$z^* = \frac{z}{a}, \quad r^* = \frac{r}{a}, \quad u^* = \frac{a}{\gamma} u, \quad p^* = \frac{pa\delta}{\rho\gamma^2}, \quad \theta^* = \frac{T - T_0}{Aa}, \quad s^* = \frac{s}{a}, \quad C^* = \frac{C - C_0}{C_i - C_0}$$

Introducing these non-dimensional variables, the governing equations in the non-dimensional form are (on removing the stars)

$$\frac{\partial^2 u}{\partial r^2} + \frac{1}{r} \frac{\partial u}{\partial r} = p + \delta(D^{-1})u + \delta^2 \Lambda u^2 - \delta G(\theta + N C) \quad (2.6)$$

$$\frac{\partial^2 \theta}{\partial r^2} + \frac{1}{r} \frac{\partial \theta}{\partial r} = P_r N_t u - \alpha - Du N_t \left( C_{rr} + \frac{1}{r} C_r \right) \quad (2.7)$$

$$\frac{\partial^2 C}{\partial r^2} + \frac{1}{r} \frac{\partial C}{\partial r} = Sc N_c u - Sc Sr \left( \theta_{rr} + \frac{1}{r} \theta_r \right) \quad (2.8)$$

where

$$\Lambda = FD^{-1} \quad (\text{Inertia parameter or Forchhimer number})$$

$$G = \frac{g\beta(T_1 - T_0)a^3}{\gamma^2} \quad (\text{Grashof number})$$

$$D^{-1} = \frac{a^2}{k} \quad (\text{Inverse Darcy parameter})$$

$$N_t = \frac{Aa}{T_1 - T_0} \quad (\text{Non-dimensional temperature gradient})$$

$$N_c = \frac{Ba}{C_1 - C_0} \quad (\text{Non-dimensional concentration gradient})$$

$$P_r = \frac{\rho c_p \gamma}{\lambda} \quad (\text{Prandtl number})$$

$$Du = \left( \frac{D_m K_t \Delta c a^2}{C_s C_p \Delta T \lambda} \right) \quad (\text{Dufour Number})$$

$$Sc = \frac{\nu}{D_m} \quad (\text{Schmidt number})$$

$$Sr = \left( \frac{D_m K_t \Delta T}{\mathcal{G} T_m \Delta C} \right) \quad (\text{Soret number})$$

With the corresponding boundary conditions are;

$$u = 0, \quad \theta = \frac{t_i - t_0}{Aa}, \quad C=1 \quad \text{at} \quad r=1 \quad (2.9)$$

$$u = 0, \quad \frac{\partial \theta}{\partial r} = Q_1, \quad C = 0 \quad \text{at} \quad r=1+s \quad (2.10)$$

### III. Finite Element Analysis

The finite element analysis with quadratic polynomial approximation functions is carried out along the radial distance across the circular cylindrical annulus. The behavior of the velocity, temperature and concentration profiles has been discussed computationally for different variations in governing parameters. The Gelarkin method have been adopted in the variational formulation in each element to obtain the global coupled matrices for the velocity, temperature and concentration in course of the finite element analysis.

The shear stress ( $\tau$ ) is evaluated using the formula:  $\tau = \left( \frac{du}{dr} \right)_{r=1,1+s}$

The rate of heat transfer (Nusselt Number) is evaluated using the formula:

$$Nu = - \left( \frac{d\theta}{dr} \right)_{r=1}$$

The rate of mass transfer (Sherwood Number) is evaluated using the formula:

$$Sh = -\left(\frac{dC}{dr}\right)_{r=1,1+s}$$

#### IV. Numerical Results

In this analysis we investigate Thermo-Diffusion and Diffusion-Thermo effects on convective heat and mass transfer flow of a viscous fluid through a porous medium in the annulus between two concentric cylinders in the presence of constant heat source and chemical reaction. The inner cylinder is maintained at constant temperature and the outer wall is maintained constant heat flux while the concentration is maintained constant on both the cylinders. In this analysis we take Prandtl number  $P=0.71$ . The axial flow is in vertically downward direction, and hence the actual axial flow ( $u$ ) is negative,  $u > 0$  indicates a reversal flow. The velocity, temperature and concentration distributions are shown in figures 1-21 for different values of the parameters  $G, D^{-1}, N, Sc, Sr, Du, \gamma$  and  $\alpha$ .

Fig. 1. represents the variation of  $u$  with Grashof number  $G$ . It is found that  $|u|$  enhances with  $G \leq 2 \times 10^3$  and depreciates with  $G \geq 5 \times 10^3$ . The variation of  $u$  with Darcy's parameter  $D^{-1}$  shows that a reversal flow appears with  $D^{-1} \geq 5 \times 10^3$  and the region of reversal flow enlarge with increase in  $D^{-1}$ . Also lesser the permeability of porous medium smaller the magnitude of  $u$  and for further lowering of the permeability larger the magnitude of  $u$  in the entire flow region (fig.2). From fig.3. We notice that for  $\alpha = 0$  a reversal flow is observed in the flow region and for  $\alpha = 2$  the flow exhibits a reversal nature and for  $\alpha = 6$  we notice a reversal flow in the flow region. The region  $1 \leq r \leq 1.6$  and for higher  $\alpha \geq 8$  the reversal flow disappears. Also  $|u|$  depreciates with  $\alpha \leq 6$  and enhances with  $\alpha \geq 8$ .

The variation of  $u$  with Schmidt number  $Sc$  indicates that lesser the molecular diffusivity larger  $|u|$  and for further lowering of molecular diffusivity it experiences an enhancement in the entire flow region (fig.4). The variation of  $u$  with Soret parameter  $Sr$  is shown in fig.5. It is found that  $|u|$  decreases with increase in  $Sr \leq 0.5$  and also decreases with  $0.5 \leq Sr \leq 1$  and it enhances with  $Sr > 1$ . The variation of  $u$  with Dufour parameter  $Du$  is shown in fig.6. We observed that the  $|u|$  experiences depreciation with increase in  $Du \leq 0.05$  and enhances with  $Du \geq 0.15$ . The variation of  $u$  with buoyancy ratio  $N$  exhibits a reversal flow with  $N = 1$  and no such reversal flow appears with any values of  $N < 0$  or  $N > 0$ . When the molecular buoyancy force dominates over the thermal buoyancy force  $|u|$  decreases irrespective of the directions of the buoyancy force (fig.7). The variation of  $u$  with chemical reaction parameter  $\gamma$  is shown in figure (7 a), from the figure we conclude that velocity increase with increase in  $\gamma$ .

The non-dimensional temperature ( $\theta$ ) is shown in fig 8- 14 for different values of the parameters  $G, D^{-1},$

$N, Sc, Sr, Du, \gamma$  and  $\alpha$ . It is found that the non-dimensional temperature is negative for all variations. This implies that the actual temperature  $\theta$  is less than that on the inner cylinder. It is found that the actual temperature enhances with increase in  $G$  with maximum at  $r = 2$  (fig.8). The variation of  $\theta$  with  $D^{-1}$  indicates that lesser the permeability of porous medium larger the actual temperature in the flow region (fig.9). The variation of  $\theta$  with heat source parameter  $\alpha$  is shown in fig.10. We observe that the actual temperature decreases with increase in  $\alpha$ . With respect to the variation of  $\theta$  with  $Sc$ , we notice that lesser the molecular diffusivity larger the actual temperature (fig. 11). The effect of Soret number  $Sr$  on  $\theta$  is shown in fig.12. It is found that higher the value of  $Sr$  larger the actual temperature in the entire flow region. From fig.14 we conclude that for smaller values of Dufour parameter  $Du$  we notice a marginal increase in the actual temperature and for higher values of  $Du \geq 0.15$  a remarkable enhancement in the actual temperature is noticed. The variation of  $\theta$  with buoyancy ratio  $N$  shows that when the molecular buoyancy force dominates over the thermal buoyancy force the actual temperature experiences an enhancement when the buoyancy forces act in the same direction while for the forces acting in opposite directions it depreciates in the flow region (fig.14). Fig (14 a) is shows the variation of  $\theta$  with chemical reaction parameter  $\gamma$ . It shows that  $\theta$  decreases with increment in  $\gamma$ .

The non-dimensional concentration ( $\phi$ ) is shown in fig 15-21 for different values of the parameters  $G, D^{-1}, N, Sc, Sr, Du, \gamma$  and  $\alpha$ . It is found that the non-dimensional concentration is positive for all variations. This indicates that the actual concentration is greater than on the inner cylinder. It is found that the actual concentration decreases with increase in  $G \leq 5 \times 10^3$  and experiences an enhancement with higher  $G \geq 10^4$  (fig.15). The variation of  $\phi$  with  $D^{-1}$  shows that lesser the permeability of porous medium smaller the actual concentration in the flow region and for further lowering of the permeability larger the actual concentration in the flow region (fig.16).

From fig. 17 we notice that an increase in the heat source parameter  $\alpha$  reduces the actual concentration in the flow region. An increase in  $\alpha \leq 6$  reduces the actual concentration in the flow and for further higher  $\alpha \geq 8$  it experiences an enhancement in the flow region with maximum at  $r = 1.6$ . With respect to the variation of  $\phi$  with  $Sc$ , we notice that lesser the molecular diffusivity larger the actual concentration in the flow region (fig.18). The influence of the Soret parameter  $Sr$  on  $\phi$  is shown in fig.19. We notice that an increase in the Soret parameter  $Sr \leq 1$  enhances the actual concentration and for higher  $Sr \geq 2$  we notice a depreciation in  $\phi$ .

The variation of  $\phi$  with  $Du$  shows that the actual concentration depreciates with increase in  $Du \leq 0.05$  and for higher  $Du \geq 0.015$  we notice an enhancement in the actual concentration (fig.20). When the molecular buoyancy force dominates over the thermal buoyancy force the actual concentration experiences an enhancement when the buoyancy forces act in the same direction while for the forces acting in opposite directions it depreciates in the flow region (fig.21). The influence of the Soret parameter  $Sr$  on  $\phi$  is shown in fig.(21a). We notice that an increase in chemical reaction parameter  $\gamma$  enhances the actual concentration in the flow region.

The shear stress ( $\tau$ ) at the inner and outer cylinders has been calculated for different values of the parameters  $G$ ,  $D^{-1}$ ,  $N$ ,  $\alpha$ ,  $Sc$ ,  $Sr$ ,  $\gamma$  and  $Du$ . These are presented in tables 1-6. It is found that the magnitude of stress enhances with an increase in Grashof number  $G$  at both cylinders. The variation of  $\tau$  with  $D^{-1}$  shows that lesser the permeability of porous medium higher  $|\tau|$  at both the cylinders. The behavior of the stress with buoyancy ratio  $N$  shows that when the molecular buoyancy force dominates over the thermal buoyancy force the magnitude of the stress experiences an enhancement at  $r=1$  and  $r=2$  irrespective of the directions of the buoyancy forces (tables 1 and 4). Variation of  $\tau$  with heat source parameter  $\alpha$  shows that  $|\tau|$  enhances with increase in  $\alpha$  at the both cylinders. Also lesser the molecular diffusivity smaller the magnitude of  $\tau$  at both cylinders (tables 2 and 5). The variation of stress with Schmidt number  $Sc$  exhibits a decreasing tendency in  $|\tau|$  at both the cylinders. The variation of  $\tau$  with Soret parameter  $Sr$  indicates that  $|\tau|$  depreciates with increase in  $Sr$ . An increase in Dufour parameter  $Du$  enhances  $|\tau|$  at  $r=1$  for all  $D^{-1}$ , while at outer cylinder  $r=2$  it depreciates with  $Du$  at  $D^{-1} = 10^3$  and enhances at higher values of  $D^{-1} \geq 5 \times 10^3$  (tables 3 and 6). In general, we notice that the stress at  $r=1$  is less than that at  $r=2$ . Variation of  $\tau$  with chemical reaction parameter  $\gamma$  shows that  $|\tau|$  enhances with increase in  $\gamma$  at the both cylinders.

The Nusslet number ( $Nu$ ) which measures the rate of heat transfer across the boundaries has been calculated for different values of the parameters  $G$ ,  $D^{-1}$ ,  $N$ ,  $\alpha$ ,  $Sc$ ,  $Sr$ ,  $\gamma$  and  $Du$  and these are presented in tables 7-9. It is found that the rate of heat transfer reduces with increase in  $G$ . The variation of  $Nu$  with  $D^{-1}$  shows that lesser the permeability of porous medium smaller the rate of heat transfer and for further lowering of the permeability it experiences an enhancement at  $r=1$ . When the molecular buoyancy force dominates over the thermal buoyancy force the magnitude of the stress experiences when the buoyancy forces act in the same direction, while for the forces acting in the opposite directions  $|Nu|$  enhances at  $r=1$  (table 7). From table 8 we notice that the rate of heat transfer enhances with increase in  $\alpha$

0. Also the variation of  $Nu$  with  $Sc$  shows that lesser the molecular diffusivity larger the rate of heat transfer (table 8). The variation of  $Nu$  with soret parameter  $Sr$  and Dufour parameter  $Du$  shows that it experiences an enhancement with increase in  $Sr$  and  $Du$  at  $r = 1$  (table 9). Variation of Nusslet number ( $Nu$ ) with chemical reaction parameter  $\gamma$  shows that  $|\tau|$  enhances with increase in  $\gamma$  at the both cylinders.

The Sherwood number ( $Sh$ ) which measures the rate of mass transfer across the cylinders has been calculated for different values of the parameters  $G$ ,  $D^{-1}$ ,  $N$ ,  $\alpha$ ,  $Sc$ ,  $Sr$ ,  $\gamma$  and  $Du$  and are presented in the tables 10-15. It is found that the rate of mass transfer experiences a depreciation at  $r=1$  and enhancement at  $r=2$  with increase in  $G$ . The variation of  $Sh$  with  $D^{-1}$  shows that lesser the permeability of porous medium smaller the rate of mass transfer at  $r=1$  and for further lowering it enhances while at  $r=2$  it experiences an enhancement. When the molecular buoyancy force dominates over the thermal buoyancy force the magnitude of the rate of mass transfer reduces at  $r=1$  and enhances at  $r=2$  when the buoyancy forces is in the same direction, while the forces acting in the opposite directions  $|Sh|$  experiences a depreciation at both cylinders (table 10 and 13). An increase in  $\alpha$  results in an enhancement at both cylinders. The variation of  $Sh$  with Schmidt number  $Sc$  exhibits that  $|Sh|$  enhances with  $Sc$  at  $r=1$ , while at  $r = 2$  it depreciates with  $Sc \leq 0.6$  and enhances with higher  $Sc \geq 2$  (tables 11 and 14). Tables 12 and 15 indicate that the variation of  $Nu$  with soret parameter  $Sr$  and Dufour parameter  $Du$  it experiences an enhancement with increase in  $Sr$  and  $Du$  at  $r = 1$  and 2. In general, we notice that the rate of mass transfer at  $r=1$  is marginally greater than that at  $r=2$ . Variation of Sherwood number ( $Sh$ ) with chemical reaction parameter  $\gamma$  shows that  $|\tau|$  enhances with increase in  $\gamma$  at the both cylinders.

## REFERENCES:

- [1]. Al Nimr MA(1993): Analytical solutions for transient laminar fully developed free convection in vertical annulus.,*Int.J.Heat and Mass Transfer*, V.36,pp.2388-2395.
- [2]. Angel M, Takhar HS, and Pop I (2000): Dofour and Soret effects on free convection boundary layer over a vertical surface embedded in a porous medium. *Studia universitates- Bolyai, Mathematica XLV*, pp. 11-21.
- [3]. Antonio Barletle(1999): Combined forced and free convection with viscous dissipation in a vertical duct.,*Int.J.Heat and Mass Transfer*,V.42,pp.2243-2253.
- [4]. Barletta A, Lazzari.S,(2008): Mixed convection with heating effects in a vertical porous annulus with a radially varying magnetic field.

- [5]. Caltirone,JP(1976):*J.Fluid Mech*,V.76,p.337.
- [6]. Chen TS and Yuh CF (1979):Combined heat and mass transfer in natural convection on inclined surface.,*J.Heat Transfer*,V.2,pp.233-250.
- [7]. Emmunuel Osalusi, Jonathan Side, Robert Harris(2008):"Thermal-diffusion and diffusion thermo effects on combined heat and mass transfer of a steady MHD convective and slip flow due to a rotating disk with viscous dissipation and ohmic heating: *Int.Communications in heat and mass transfer*,Vol.35,PP.908-915.
- [8]. Faces N and Faroup B (1983):*ASME,J.Heat Transfer*,V.105,p.680.
- [9]. Havstad MA and Burns PJ(1982): *Int.J.Heat&Mass Transfer*, V.25,No.1, p.1755.
- [10]. Lakshmi Narayana PA. et al (2007): Soret and Dufour effects in a doubly stratified Darcy porous medium, *Journal of a porous medium* 10. pp 613-624.
- [11]. Lakshmi Narayana PA and Murthy PVSN (2008): Soret and Dufour effects on free convection heat and mass transfer from horizontal flat plate in a Darcy porous medium. *Journal of heat transfer* 130. 104504-1-104504-5.
- [12]. Mansour A et al (2006): Multiplicity of solutions induced by thermosolutal convection in a porous squire cavity heated from below and submitted to horizontal concentration gradient in the presence of Soret effect, *Numerical Heat Transfer , Part A*, Applications 49, pp 69-94.
- [13]. Mihirsen, Torrance KE (1987): *Int.J.Heat and Mass Transfer* ,V.30, No.4,p. 729.
- [14]. Nanda RS and Prushotham R (1976) : Int.dedication seminar on recent advances on maths and applications, Vaeanasi.
- [15]. Neeraja,G(1993):Ph.D thesis,S.P.Mahila University,Tirupathi,India.
- [16]. Nguyen TH, Saish MG, Robillard and Vasseur P (1985):ASME,The American Society of Mechanical Enginners,Paper No.85-WA/HT-8,New York.
- [17]. Osterle JF and Young FJ (1961) :*J.Fluid Mech*.,V.11,p.512.
- [18]. Partha MK, Murthy PVSN, Rajashekar GP (2006): Soret and dufour effects in a non-Darcy porous medium,*Journal of heat and mass transfer*.V.128. pp 605-610.
- [19]. Postelnicu A (2004): Influence of magnetic field on heat and mass transfer by natural convection from vertical surface in a porous media considering Soret and Dufour effects. *Int.J. of heat and mass transfer*, V.47, Pp 1467-1472.
- [20]. Philip JR(1982): Axisymmetric free convection at small Rayleigh numbers in porous cavities, *Int. J. Heat and Mass Transfer*,V.25,pp.1689-1699.
- [21]. Poots G(1961): *Int.J.Heat and Mass Transfer* ,V.3,p.1.
- [22]. Prasad V(1983): Natural convection in porous media ,Ph.D thesis ,S. K. University, Anantapur, India.
- [23]. Prasad V and Kulacki FA(1984): *Int.J.Heat and Mass Transfer*,V.27,p.207.
- [24]. Prasad V, Kulacki FA and KeyhariM (1985): *J.Fluid Mech*.,V.150,p.89.
- [25]. Rani A (2003): Unsteady convection heat and mass transfer flow through a porous medium in wavy channels.,Ph.D thesis,S.K.University,Anantapur,India.
- [26]. Rao YF, MikimY, Fukuda Takata Y and Hasegahea S(1985): *Int.J.Heat and Mass Transfer*, V.28,p.705.
- [27]. Robillard L, Ngugen TH, Sathish MG and Vasseur P (1985): Heat transfer in porous media and particulate flows, *HTD-V.46,p.41.ASME*.
- [28]. Sastri VUK and Bhadram CVV(1978) : *App,Sci.Res*,V.34,2/3.p.117.
- [29]. Shaarawi El MAI and Al-Nimir MA(1995): Fully developed laminar natural convection in open ended vertical concentric annulus. *Int. J. Heat and Mass Transfer* ,pp.1873-84.
- [30]. Singh KR and Cowling TJ (1963) : *Quart.J.Maths.Appl.Maths*,V.16.p.1.
- [31]. Sivanjaneta Prasad P(2001): Effects of convection heat and mass transfer in unsteady hydromagnetic channels flow, Ph.D thesis, S.K.University, Anantapur,India.
- [32]. Sreenivas Reddy B (2006): Thermo-diffusion effect on convection heat and mass transfer through a porous medium,Ph.D thesis,S.K.University,Anantapur,India.
- [33]. Sreevani M (2003): Mixed convection heat and mass transfer through a porous medium in channels with dissipative effects,Ph.D thesis ,S,K.University, Anantpur.
- [34]. Sudeer Kumar Nguyen TH ,Robillard and Thi VKT(1984): *Int.Heat and m,ass transfer* ,V.27, p.337.
- [35]. Whitehead JA (1972): Observations of rapid means flow produced mercury by a movingheater,Geophys. *Fluid dynamics*, V.3, pp.161-180.
- [36]. Yu CP (1970):*Appl.Sci.Res*, V.22, p.127.
- [37]. Yu CP and Yong,H(1969): *Appl.Sci.Res*,V.20,p.16.

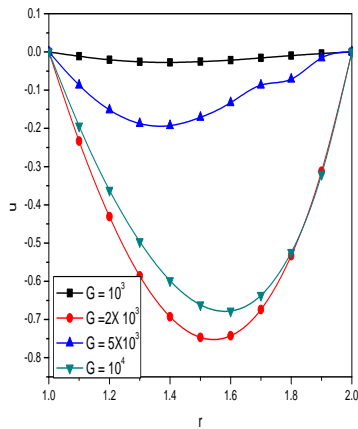


Fig.1 Variation of u with G  
 $P=0.71, Sr=0.5, D^{-1}=2 \times 10^3, N=1, Sc=1.3, \alpha=2,$   
 $Du=0.05$

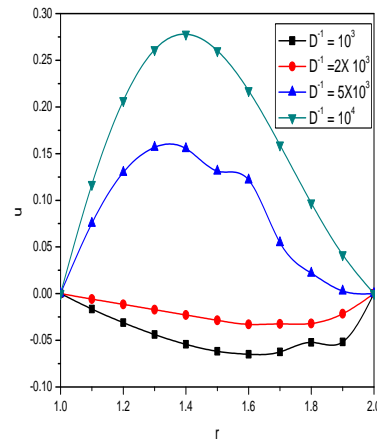


Fig.2 Variation of u with  $D^{-1}$   
 $P=0.71, Sr=0.5, G=2 \times 10^3, Sc=1.3, \alpha=2, N=1, Du=0.05.$

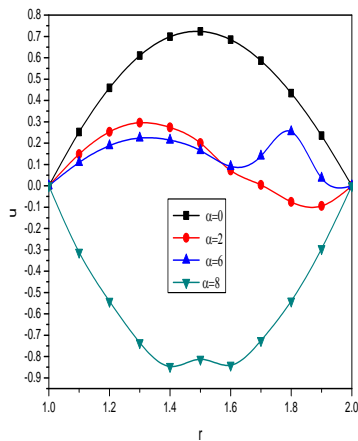


Fig.3. Variation of u with  $\alpha$   
 $P=0.71, Sr=0.5, D^{-1}=2 \times 10^3, Sc=1.3, G=2 \times 10^3, N=1, Du=0.05.$

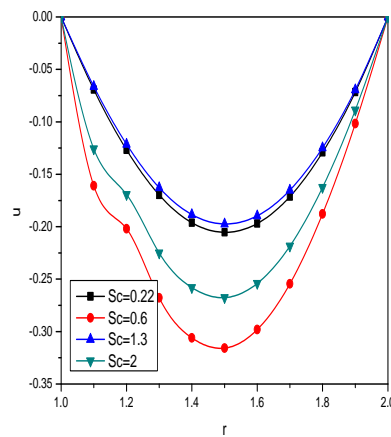


Fig.4. Variation of u with Sc  
 $P=0.71, Sr=0.5, G=2 \times 10^3, D^{-1}=2 \times 10^3, N=1, \alpha=2, Du=0.05.$

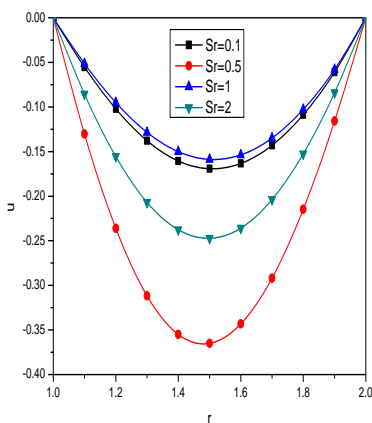


Fig 5. Variation of u with Sr  
 $P=0.71, D^{-1}=2 \times 10^3, Sc=1.3, \alpha=2, G=2 \times 10^3, N=1, Du=0.05.$

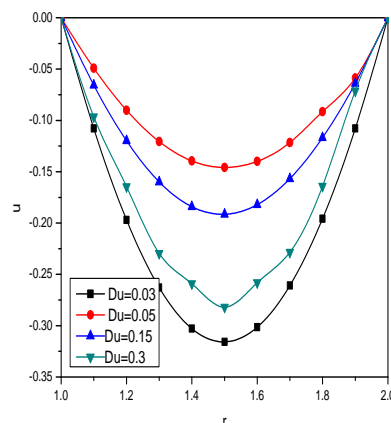


Fig 6. Variation of u with Du  
 $P=0.71, Sr=0.5, G=2 \times 10^3, D^{-1}=2 \times 10^3, N=1, Sc=1.3, \alpha=2$



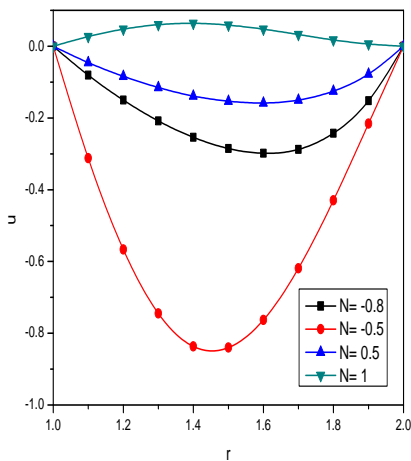


Fig7. Variation of u with N

$P=0.71, Sr=0.5, D^{-1}=2 \times 10^3, G=2 \times 10^3, Sc=1.3, \alpha=2, Du=0.05.$

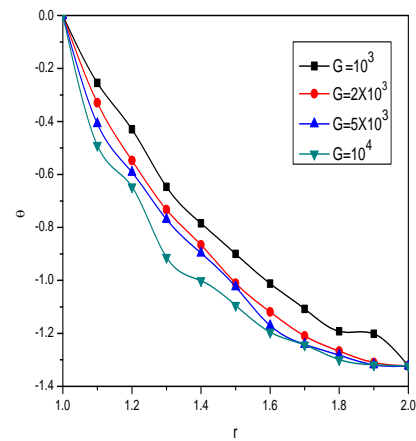


Fig8. Variation of u with G

$P=0.71, Sr=0.5, D^{-1}=2 \times 10^3, N=1, Sc=1.3, \alpha=2, Du=0.05$

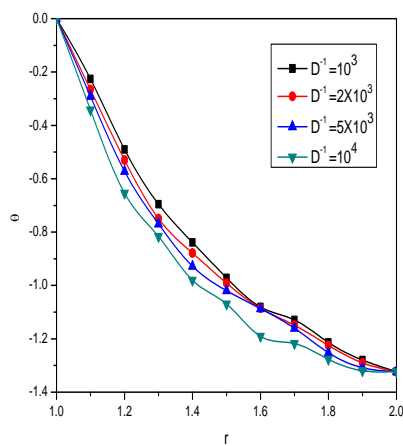


Fig9. Variation of u with  $D^{-1}$

$P=0.71, Sr=0.5, G=2 \times 10^3, Sc=1.3, \alpha=2, N=1, Du=0.05$

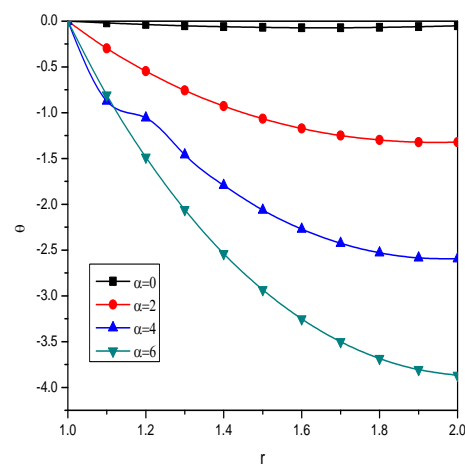


Fig10. Variation of  $\theta$  with  $\alpha$

$P=0.71, Sr=0.5, D^{-1}=2 \times 10^3, Sc=1.3, G=2 \times 10^3, N=1, Du=0.05.$

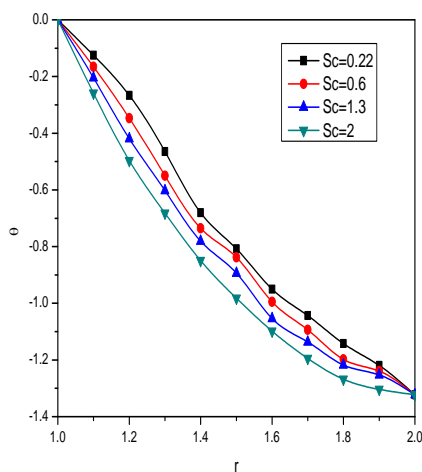


Fig11. Variation of  $\theta$  with Sc

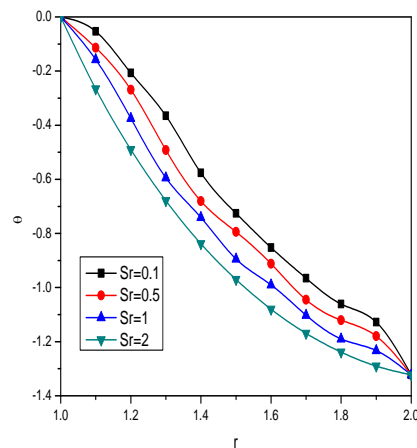


Fig12. Variation of  $\theta$  with Sr

$P=0.71, D^{-1}=2 \times 10^3, Sc=1.3, \alpha=2, G=2 \times 10^3, N=1, Du=0.05.$

$P=0.71, Sr=0.5, G=2 \times 10^3, D^{-1}=2 \times 10^3, N=1, \alpha=2, Du=0.05$

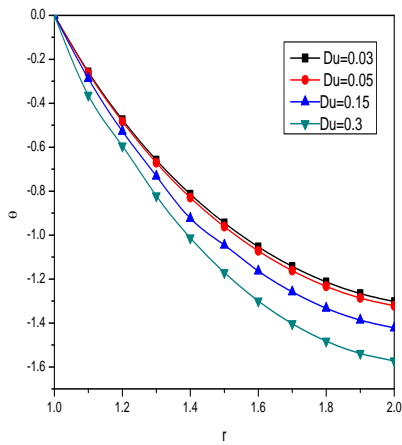


Fig.13.Variation of  $\theta$  with  $Du$   
 $P=0.71, Sr=0.5, G=2 \times 10^3, D^{-1}=2 \times 10^3, N=1, Sc=1.3, \alpha=2$

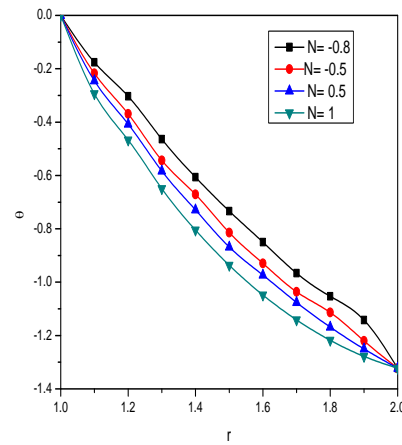


Fig.14. Variation of  $\theta$  with  $N$   
 $P=0.71, Sr=0.5, D^{-1}=2 \times 10^3, G=2 \times 10^3, Sc=1.3, \alpha=2, Du=0.05$

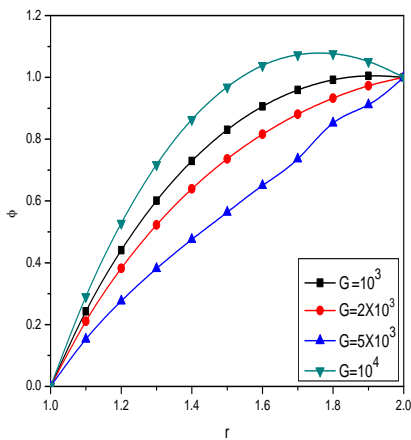


Fig.15. Variation of  $u$  with  $G$   
 $P=0.71, Sr=0.5, D^{-1}=2 \times 10^3, N=1, Sc=1.3, \alpha=2, Du=0.05$

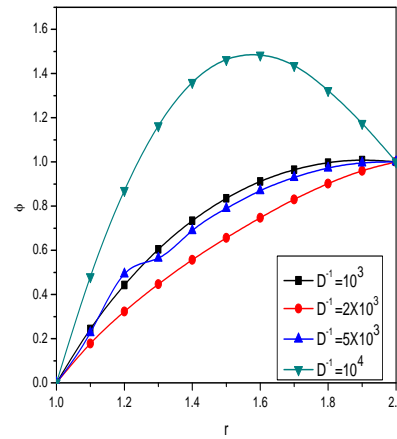


Fig.16.Variation of  $u$  with  $D^{-1}$   
 $P=0.71, Sr=0.5, G=2 \times 10^3, Sc=1.3, \alpha=2, N=1, Du=0.05$

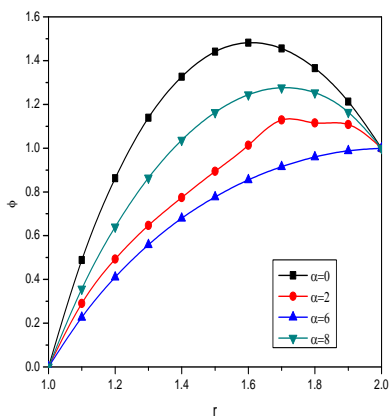


Fig.17.Variation of  $\phi$  with  $\alpha$   
 $P=0.71, Sr=0.5, D^{-1}=2 \times 10^3, Sc=1.3, G=2 \times 10^3, N=1, Du=0.05$

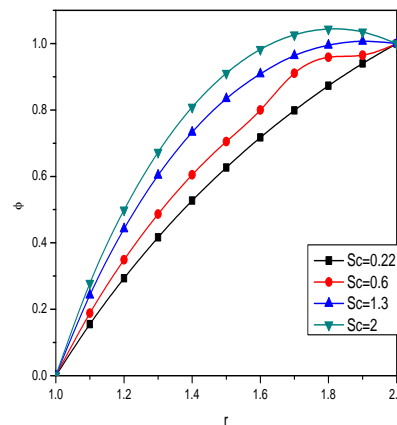


Fig.18.Variation of  $\phi$  with  $Sc$   
 $P=0.71, Sr=0.5, G=2 \times 10^3, D^{-1}=2 \times 10^3, N=1, \alpha=2, Du=0.05$

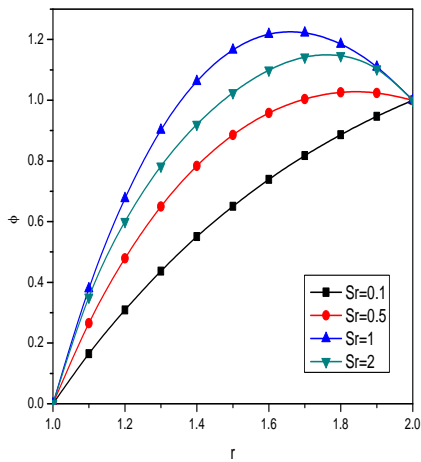


Fig.19. Variation of  $\Phi$  with Sr  
 $P=0.71, D^{-1}=2 \times 10^3, Sc=1.3, \alpha=2, G=2 \times 10^3, N=1, Du=0.05.$

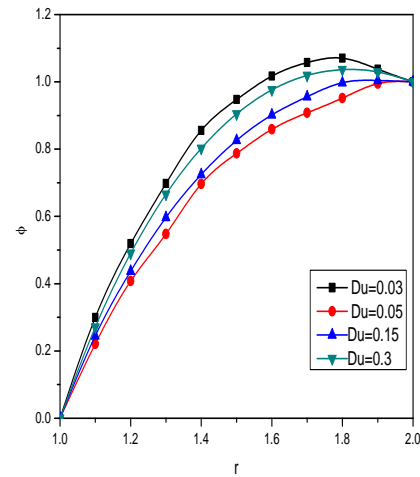


Fig.20. Variation of  $\Phi$  with Du  
 $P=0.71, Sr=0.5, G=2 \times 10^3, D^{-1}=2 \times 10^3, N=1, Sc=1.3, \alpha=2$

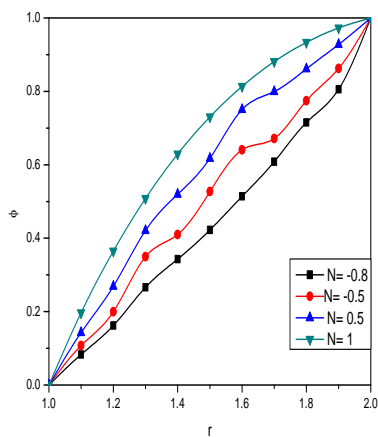


Fig.21. Variation of  $\Phi$  with N  
 $P=0.71, Sr=0.5, D^{-1}=2 \times 10^3, G=2 \times 10^3, Sc=1.3, \alpha=2, Du=0.05.$

Table-1

Shear Stress ( $\tau$ ) at  $r=1$ .

$P=0.71, Sr=0.5, Sc=1.3, \alpha=2, Du=0.05.$

$D^{-1}$	I	II	III	IV	V	VI	VII
$10^3$	-0.358119	-1.61797	-2.8824	-1.7676	-1.45497	1.2569	1.5699
$5 \times 10^3$	-1.88788	-3.59939	-5.78854	-4.18923	-3.58156	2.3569	2.8974
$10^4$	1.55733	11.5689	60.7597	7.21284	6.34167	5.2369	5.5879
G	$10^3$	$5 \times 10^3$	$10^4$	$2 \times 10^3$	$2 \times 10^3$	$2 \times 10^3$	$2 \times 10^3$
N	2	2	2	-0.8	-0.5	2	2
$\gamma$	1	1	1	1	1	1	3

**Table-2**  
**Shear Stress ( $\tau$ ) at  $r=1$ .**  
 **$P=0.71, Sr=0.5, G=2X10^3, N=1, Du=0.05$ .**

$D^{-1}$	I	II	III	IV	V	VI
$10^3$	0.320322	-1.71519	-2.73294	-0.813004	-0.774916	-0.608707
$5x10^3$	0.780488	-4.13658	-6.59511	-1.83393	-1.7843	-1.54678
$10^4$	-1.60363	8.3765	13.3666	4.85912	4.29259	2.62289
$\alpha$	0	4	6	2	2	2
Sc	1.3	1.3	1.3	0.22	0.6	2

**Table-3**  
**Shear Stress ( $\tau$ ) at  $r=1$ .**  
 **$P=0.71, G=2X10^3, \alpha=2, N=1, Sc=1.3$ .**

$D^{-1}$	I	II	III	IV	V	VI
$10^3$	-0.80333	-0.528069	0.0397044	-0.39989	-0.41652	1.00831
$5x10^3$	-1.80258	-1.44559	-0.135859	-1.6399	-1.86913	-2.15807
$10^4$	4.9552	2.0005	0.25157	3.292	3.89233	4.83277
Sr	0.1	1	2	0.5	0.5	0.5
Du	0.05	0.05	0.05	0.03	0.15	0.3

**Table-4**  
**Shear Stress ( $\tau$ ) at  $r=2$ .**  
 **$P=0.71, Sr=0.5, Sc=1.3, \alpha=2, Du=0.05$ .**

$D^{-1}$	I	II	III	IV	V	VI	VII
$10^3$	0.3796	1.77518	3.29787	1.99225	1.92493	1.3651	1.40258
$5x10^3$	0.74348	3.15052	5.34226	3.57134	3.05634	1.9871	2.0145
$10^4$	-0.853107	-6.78115	-38.4785	-3.8659	-3.4171	2.0458	2.6501
G	$10^3$	$5X10^3$	$10^4$	$2X10^3$	$2X10^3$	$2X10^3$	$2X10^3$
N	2	2	2	-0.8	-0.5	2	2
$\nu$	1	1	1	1	1	1	3

**Table-5**  
**Shear Stress ( $\tau$ ) at  $r=2$ .**  
 **$P=0.71, Sr=0.5, G=2 \times 10^3, N=1, Du=0.05$ .**

$D^{-1}$	I	II	III	IV	V	VI
$10^3$	-0.36612	1.85787	2.96986	0.82371	0.79805	0.68618
$5 \times 10^3$	-0.684885	3.5278	5.63321	1.5256	1.49232	1.3334
$10^4$	0.86962	-4.6445	-7.4015	-2.86145	-2.4867	-1.38263
$\alpha$	0	4	6	2	2	2
Sc	1.3	1.3	1.3	0.22	0.6	2

**Table-6**  
**Shear Stress ( $\tau$ ) at  $r=2$ .**  
 **$P=0.71, G=2 \times 10^3, \alpha=2, N=1, Sc=1.3$ .**

$D^{-1}$	I	II	III	IV	V	VI
$10^3$	0.81716	0.632059	0.25173	0.53923	0.52466	-0.2289
$5 \times 10^3$	1.50462	1.26576	0.394923	1.3884	1.58514	1.83258
$10^4$	-2.92492	-0.97128	0.18333	-1.83352	-2.17959	-2.73827
Sr	0.1	1	2	0.5	0.5	0.5
Du	0.05	0.05	0.05	0.03	0.15	0.3

**Table-7**  
**Nusslet Number (Nu) at  $r=1$ .**  
 **$P=0.71, Sr=0.5, Sc=1.3, \alpha=2, Du=0.05$ .**

$D^{-1}$	I	II	III	IV	V	VI	VII
$10^3$	-2.99512	-2.52163	-2.04544	-2.59865	-2.14536	2.0568	2.3265
$5 \times 10^3$	-2.79583	-1.77626	-0.9487	-1.58922	-1.7969	3.1568	3.2145
$10^4$	-3.7158	-7.48267	-25.042	-5.4437	-5.07468	3.9658	3.9871
G	$10^3$	$5 \times 10^3$	$10^4$	$2 \times 10^3$	$2 \times 10^3$	$2 \times 10^3$	$2 \times 10^3$
N	2	2	2	-0.8	-0.5	2	2
$\nu$	1	1	1	1	1	1	3

**Table-8**  
**Nusslet Number (Nu) at r=1.**  
**P=0.71, Sr=0.5, G=2X10<sup>3</sup>, N=1, Du=0.05.**

D <sup>-1</sup>	I	II	III	IV	V	VI
10 <sup>3</sup>	-0.19211	-5.54307	-8.21855	-2.7711	-2.80297	-2.9413
5x10 <sup>3</sup>	-0.36522	-4.6322	-6.76566	-2.40522	-2.43512	-2.5768
10 <sup>4</sup>	0.53188	-9.34009	-14.276	-4.80399	-4.6498	-4.1983
α	0	4	6	2	2	2
Sc	1.3	1.3	1.3	0.22	0.6	2

**Table-9**  
**Nusslet Number (Nu) at r=1.**  
**P=0.71, G=2X10<sup>3</sup>, α =2, N=1, Sc=1.3.**

D <sup>-1</sup>	I	II	III	IV	V	VI
10 <sup>3</sup>	-2.7787	-3.00855	-3.47362	-2.99399	-4.15624	-17.6093
5x10 <sup>3</sup>	-2.4226	-2.6376	-3.39023	-2.46537	-2.67155	-2.96102
10 <sup>4</sup>	-4.8312	-4.03105	-3.57449	-4.27739	-5.15322	-6.80577
Sr	0.1	1	2	0.5	0.5	0.5
Du	0.05	0.05	0.05	0.03	0.15	0.3

**Table-10**  
**SherWood Number (Sh) at r=1.**  
**P=0.71, Sr=0.5, Sc=1.3, α=2, Du=0.05.**

D <sup>-1</sup>	I	II	III	IV	V	VI	VII
10 <sup>3</sup>	2.88708	2.36217	1.83605	0.839418	1.91976	2.3651	2.3981
5x10 <sup>3</sup>	2.66259	1.52294	0.60197	1.66993	1.809	2.8024	2.9125
10 <sup>4</sup>	3.70126	7.9647	27.7927	1.89519	3.09037	3.1045	3.3451
G	10 <sup>3</sup>	5X10 <sup>3</sup>	10 <sup>4</sup>	2X10 <sup>3</sup>	2X10 <sup>3</sup>	2X10 <sup>3</sup>	2X10 <sup>3</sup>
N	2	2	2	-0.8	-0.5	2	2
γ	1	1	1	1	1	1	3

**Table-11**  
**SherWood Number (Sh) at r=1.**  
**P=0.71, Sr=0.5, G=2X10<sup>3</sup>, N=1, Du=0.05.**

D <sup>-1</sup>	I	II	III	IV	V	VI
10 <sup>3</sup>	1.56795	3.92316	5.10077	1.63659	2.00325	3.59005
5x10 <sup>3</sup>	1.76287	2.89726	3.46446	1.56738	1.81297	2.95484
10 <sup>4</sup>	0.74008	8.21246	11.9437	2.02215	2.9612	5.78602
α	0	4	6	2	2	2
Sc	1.3	1.3	1.3	0.22	0.6	2

**Table-12**  
**SherWood Number (Sh) at r=1.**  
**P=0.71, G=2X10<sup>3</sup>, α=2, N=1, Sc=1.3.**

D <sup>-1</sup>	I	II	III	IV	V	VI
10 <sup>3</sup>	1.72041	4.3622	9.63269	5.26821	8.61007	13.2599
5x10 <sup>3</sup>	1.69302	3.45777	9.2111	2.32145	2.38125	2.49742
10 <sup>4</sup>	1.88404	6.85941	10.1456	4.34597	5.22368	7.04582
Sr	0.1	1	2	0.5	0.5	0.5
Du	0.05	0.05	0.05	0.03	0.15	0.3

**Table-13**  
**SherWood Number (Sh) at r=2.**  
**P=0.71, Sr=0.5, Sc=1.3, α=2, Du=0.05.**

D <sup>-1</sup>	I	II	III	IV	V	VI	VII
10 <sup>3</sup>	-0.39275	0.42062	0.893403	0.97931	14.2781	2.0145	2.1365
5x10 <sup>3</sup>	-0.53922	0.801438	1.76118	0.247188	0.350403	2.5014	2.6589
10 <sup>4</sup>	-0.910097	-3.37243	-15.966	2.79928	3.57284	3.0125	3.2014
G	10 <sup>3</sup>	5X10 <sup>3</sup>	10 <sup>4</sup>	2X10 <sup>3</sup>	2X10 <sup>3</sup>	2X10 <sup>3</sup>	2X10 <sup>3</sup>
N	2	2	2	-0.8	-0.5	2	2
γ	1	1	1	1	1	1	3

**Table-14**  
**SherWood Number (Sh) at r=2.**  
**P=0.71, Sr=0.5, G=2X10<sup>3</sup>, N=1, Du=0.05.**

D <sup>-1</sup>	I	II	III	IV	V	VI
10 <sup>3</sup>	0.558819	-1.02293	-1.8138	0.572949	0.306248	-0.84192
5x10 <sup>3</sup>	0.424227	-0.518374	-0.689675	0.620335	0.436589	0.605332
10 <sup>4</sup>	1.07734	-3.7521	-6.16682	0.325314	-0.3074	-2.22902
α	0	4	6	2	2	2
Sc	1.3	1.3	1.3	0.22	0.6	2

**Table-15**  
**SherWood Number (Sh) at r=2.**  
**P=0.71, G=2X10<sup>3</sup>, α =2, N=1, Sc=1.3.**

D <sup>-1</sup>	I	II	III	IV	V	VI
10 <sup>3</sup>	0.510311	-1.39419	-5.12372	-2.04802	-4.34759	-18.6276
5x10 <sup>3</sup>	0.52798	-0.770546	-4.77854	0.0572406	0.0773228	-0.13047
10 <sup>4</sup>	0.42246	-2.96695	-5.28501	-1.26002	-1.81017	-2.9728
Sr	0.1	1	2	0.5	0.5	0.5
Du	0.05	0.05	0.05	0.03	0.15	0.3